GA–A23431

IMPROVED CCD DETECTORS FOR THE EDGE CHARGE EXCHANGE SPECTROSCOPY SYSTEM ON THE DIII–D TOKAMAK

by
K.H. BURRELL, D.H. KAPLAN, P. GOHIL,
D.G. NILSON, R.J. GROEBNER, and D.M. THOMAS

AUGUST 2000

DISCLAIMER

GA–A23431

IMPROVED CCD DETECTORS FOR THE EDGE CHARGE EXCHANGE SPECTROSCOPY SYSTEM ON THE DIII–D TOKAMAK

by
K.H. BURRELL, D.H. KAPLAN, P. GOHIL,
D.G. NILSON,* R.J. GROEBNER, and D.M. THOMAS

This is a preprint of a paper presented at the Thirteenth Topical Conference on High Temperature Diagnostics, June 18–22, 2000 in Tucson, Arizona, and to be published in *Rev. Sci. Instrum.*

*Lawrence Livermore National Laboratory, Livermore, California.

Work supported by
the U.S. Department of Energy
under Contract No. DE-AC03-99ER54463

GA PROJECT 30033
AUGUST 2000

ABSTRACT

Charge exchange spectroscopy is one of the key ion diagnostics on the DIII–D tokamak. It allows measurement of impurity densities, toroidal and poloidal rotation speeds, ion temperatures and the radial electric field. For the 2000 experimental campaign, we have replaced the intensified photodiode array detectors on the edge portion of the system with advanced charge-coupled device (CCD) detectors mounted on faster (f/4.7) Czerny-Turner spectrometers equipped with toroidal mirrors. The combination has improved the photoelectron signal level by about a factor of 20 and the signal to noise by a factor of 2 to 8, depending on the absolute signal level and readout mode. A major portion of the signal level improvement comes from the improved quantum efficiency of the back-illuminated, thinned CCD detector (70% to 85% quantum efficiency for the CCD versus 10% for the image intensifier) with the remainder coming from the faster spectrometer. The CCD camera also allows shorter minimum integration times: 0.33 ms while archiving to computer memory and 0.15 ms using temporary storage on the CCD chip.

INTRODUCTION

Charge exchange excitation of spectral lines in tokamak plasmas was discovered almost 25 years ago.[1] Since then, it has become the basis for one of the standard ion diagnostic techniques on magnetic fusion devices equipped with neutral beam injection.[2–15] Using Doppler broadening and Doppler shift of the excited spectral lines, charge exchange recombination (CER) spectroscopy produces information on the ion temperature T_i, toroidal rotation speed V_ϕ, and poloidal rotation speed V_θ of the ionic species being measured. In addition, coupling the line intensity with neutral beam deposition calculations[8] provides information on the number density n_I of the impurity measured. Furthermore, combining these measurements with the radial force balance equation[9,17–19] allows calculation of the radial electric field E_r. Finally, measurements of the intensity of the D_α radiation from the neutrals in the beam can provide a check on the beam deposition calculation.[6]

For more than a decade, the multichord edge CER system on DIII–D has been used as part of our program of edge physics studies, especially studies of the L to H transition,[9,17–19] the H–mode edge transport barrier, the H–mode edge pedestal[20] and the behavior of edge localized modes. The ability to determine the edge E_r profile with fast time resolution and high spatial resolution has been essential in testing and developing the model of E×B shear stabilization of turbulence.[9,17–19] This system, which has 8 vertical and 8 poloidal views spanning 4.3 cm at the plasma edge, initially utilized detectors based on microchannel plate image intensifiers and silicon linear photodiode arrays. The detectors were mounted on spectrometers which receive their light from the tokamak through 16 pairs of optical fibers. The minimum time resolution was 0.52 ms, set by the readout time of the 1024 diode linear arrays. This was barely adequate, for example, to investigate the time evolution of E_r across the L to H transition[18,19] or to study edge parameter variation during edge localized modes. Depending on the light level, the decay time of the P-20 phosphor in the intensifiers could also increase the minimum effective time resolution.

The goal of the present work was to upgrade the edge CER system on DIII–D so that minimum integration times significantly below 0.52 ms could be attained while increasing the total signal level enough that such short integration times would actually have usable signal to noise levels. Reaching this goal required upgrading both the photodetectors and the spectrometers. The work presented here is a continuation of the development reported previously.[21] For the 2000 experimental campaign, we have replaced the intensified photodiode array detectors on the edge portion of the system with advanced charge-coupled device (CCD) detectors[22] mounted on faster (f/4.7) Czerny-Turner spectrometers[23] equipped with toroidal mirrors. The combination has improved the photoelectron signal level by about a factor of 20 and the signal to noise by a factor

of 2 to 8, depending on the absolute signal level and readout mode. A major portion of the signal level improvement comes from the improved quantum efficiency of the back-illuminated, thinned CCD detector (70% to 85% quantum efficiency for the CCD versus 10% for the image intensifier) with the remainder coming from the faster spectrometer. The CCD camera also allows shorter minimum integration times: 0.33 ms while archiving to computer memory and 0.15 ms using temporary storage on the CCD chip.

I. DESIGN PHILOSOPHY AND CHOICES

The basic design choices have been discussed previously.[21] They lead us to a design with four f/4.7 Czerny-Turner spectrometers for the 16 pairs of optical fibers which conduct light to the spectrometers from the 16 view locations in the tokamak. Although more specialized designs with greater light gathering power have been created since our original choices were made,[16] the DIII–D experimentalists' need for broad wavelength coverage and ease of setting wavelengths between shots constrains us to continue using standard spectrometers.[23] For example, edge plasma studies on DIII–D require a CER system which can cover a broad wavelength range in order to view various lines from various impurities that are of interest (e.g. D I 656.2 nm, He II 468.57 nm, B V 494.47 nm, C VI 343.37 nm, C VI 529.05 nm, C VI 771.68 nm, Ne X 524.90 nm, Ar XVI 346.3 nm, Ar XVIII 344.9 nm). Our spectrometers also have the dispersion necessary to work in the tokamak plasma edge, where temperatures in the range of 0.1 to 1 keV and rotation speeds of order 10 km/s must be measured.

Although the logic which lead to high speed CCDs for the detectors remains sound, our previous choice of detectors[21] did not allow us to achieve the low read noise required for the highest speed. In spite of an extensive development program, the best read noise that we could achieve from the VCCD512 was about 75 electrons at a digitizing rate of 1.1 MHz, significantly above the 35–45 electrons quoted in the published specifications.[24] While this was insufficient for a high speed, edge measurements, this read noise is quite adequate for the 5–10 ms integration times typically used for core measurements; two of the spectrometer and detector systems discussed previously[21] have been used for those purposes for the past four years. Having these extra spectrometers and detector systems has been quite important for impurity transport studies in high performance discharges.[25,26]

Fortunately, the state of the art in commercial, high-speed scientific CCD cameras had advanced far enough by 1997 that detectors beyond the VCCD512[24] were available. Indeed, these are now contained in complete camera systems which include all the control circuitry and digitizers. An extensive search of available systems turned up the Pluto camera by PixelVision of Oregon[22] which contains a 652×488 pixel chip from Scientific Imaging Technologies (SITe) with split frame architecture, frame transfer readout, and four readout amplifier chains. In other words, each quadrant of the chip is read out separately, which speeds up the overall readout by a factor of four. The chip itself is capable of a minimum parallel row transfer time of 0.4 microsecond although the existing control electronics are limited to 0.6 microseconds. The chip is back-illuminated and thinned, which has a significant advantage in quantum efficiency, as

is illustrated in Fig. 1. This increase in quantum efficiency is crucial for high speed applications, which are almost always photon starved. The pixels on the chip are square, 12 microns on a side.

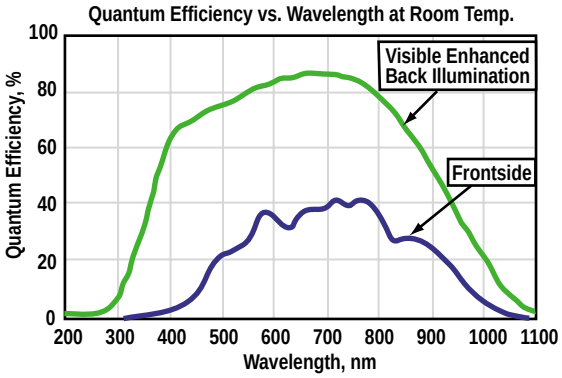

Fig. 1. Comparison of quantum efficiency as a function of wavelength between back-illuminated and front-illuminated CCD chips from Scientific Imagining Technologies (SITe).

The Pluto camera itself contains the CCD chip and all the associated control and digitizing electronics. DC power is provided by a separate power supply module. The CCD chip temperature is feedback regulated using a thermoelectric cooler (TEC) at software selectable temperatures between 220 Kelvin and 300 Kelvin; use of water chilled to 10°C to cool the TEC output is necessary to reach temperatures below 240 Kelvin. The data produced by the camera are coupled to a personal computer (PC) via fiber optic data links. Software on the PC controls the camera and allows display of the data. Our system runs under Windows NT 4.0.

A major issue in creating a high speed CCD system is the increase of readout noise with readout speed. This scales as $f^{1/2}$, where f is the readout frequency. One way around this that has been used in the past has been to create a burst mode type of high speed operation where some spectra are acquired in a short time interval, temporarily stored on the chip and then read out at a slow speed to improve the readout noise. Frame transfer chips are especially suited to such a mode of operation because they have separate exposure and storage CCD regions each of which can be independently clocked. Accordingly, each spectrum from the exposure region can be binned on to one row of the storage region; consequently, as many spectra can be stored as there are storage rows. For the Pluto 652×488 chip this amounts to about 250 spectra on each half of the chip. At the minimum parallel row transfer time of 0.6 microseconds, this gives a minimum integration time of 152 microseconds. After the storage area is full, the spectra are read out one at a time at a 0.5 MHz digitizing rate. The measured system plus CCD readout noise is about 15 electrons in this mode, which is a factor of five better than we achieved with the VCCD512 CCDs.

This sample mode of operation with intermediate on-chip storage is suitable for only a small fraction of the experiments on DIII–D. Most experimentalists need more than 250 timeslices per shot and do not require the 0.15 ms minimum integration time. The Pluto camera contains a flexible digital signal processing system with storage for up to eight different readout programs stored in programmable read only memory (PROM) pages which are accessible through software commands. (There was only one PROM program in our previous CCD system, which greatly limited flexibility.) One of these programs is the so-called TDI mode. The name is based on the

program's resemblance to the time-delayed integration mode used in some CCD cameras to track moving images. In this mode, the 251 rows of the exposure area are transferred to the storage area at the same time that the 251 rows of the storage areas are binned on to the serial register. The serial register is then read out. We chose to read out the serial register at the maximum, 2.2 MHz rate at which the cameras' 14 bit digitizers can transfer data to PC memory. This leads to a minimum integration time of 0.33 ms in this mode of operation. The advantage of TDI mode is that the number of spectra acquired during a shot is not limited by the size of the storage area on the chip. At present, we typically acquire 750 timeslices during one shot; however, the only practical limit on this number is the amount of memory on the PC. With two CCD cameras on one PC running Windows NT 4.0 and having 128 MByte of memory, we have acquired 4096 timeslices per camera per shot. Because of our choice of 2.2 MHz digitizing rate, the readout noise for TDI mode is about 30 electrons, which is still a factor of 2.5 better than our previous system. In principle, one could program a TDI mode with 0.5 MHz digitizing rate, which would give 15 electrons readout noise but limit the minimum integration time to 0.84 ms.

Another advantage to the multiple PROM pages in the Pluto camera is the ability to run the camera as a standard, two-dimensional imager. When doing the initial alignment of the camera to the spectrometer, being able to actually see the image of the fiber tips on the camera makes this process much more straightforward. Indeed, the software on the PC provides a repetitive readout mode which allows one to view in real time the changes in the image as the camera is moved relative to the spectrometer.

Coupling of the cameras to the spectrometers was the key challenge in the present design. Our initial desire was to use a 1024×1024 Pluto CCD chip, which has been in development over the past several years. This chip is large enough that four spectra could have been focused directly on the chip by the spectrometer; we would have needed one camera per spectrometer, just as with our previous system.[21] Unfortunately, this chip is not yet available in commercial quantities and it is no longer clear that it will ever be available. The 652×488 Pluto chip has been available for some time; however, this chip is significantly smaller, having about 1/3 the area. We looked extensively at various optical systems which would have allowed us to shrink the image at the spectrometer exit plane down to fit the smaller chip. However, given the broad wavelength range that our system must cover (at least 300 nm to 800 nm), the fast f/number of the spectrometer and the blurring constraints imposed by the spectral resolution required, the only lens systems we were able to devise were extremely costly and difficult to align. For instance, one design had nine lenses with eight of them independently movable for work at different wavelengths. Different lens systems with different anti-reflection coatings would have been needed for different parts of the wavelength range.

Faced with lens systems whose costs would exceed the cost of extra Pluto cameras, we decided to reduce the number of spectra per camera from four to two and double the number of

cameras. In order to position two cameras on one spectrometer, we devised the design shown in Fig. 2. Here, two planar mirrors are inserted in the optical path. The first directs the light from the spectrometer upwards through a hole bored in the hatch cover of the spectrometer. The second sends the light to one camera or the other. The spacing of the four pairs of fibers on the entrance slit is chosen so that the two faces of the second mirror each intercept light from only two of the pairs of fibers. The cameras are mounted nose to nose, which is the only way to get the two CCD chips close enough to each other that all four pairs of fibers can be kept close to the optical axis of the spectrometer.

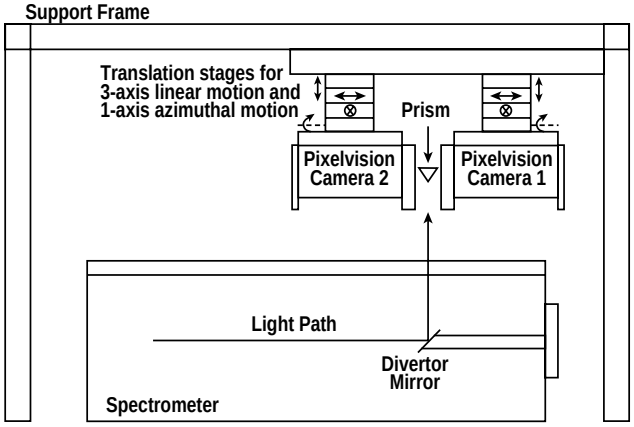

Fig. 2. Side view of AM506 spectrometer showing extra mirrors added to couple light from the spectrometer to two CCD cameras mounted on top of the spectrometer. The mount includes three axis linear translation plus rotation about the long axis of the camera. These adjustments allow the camera to be aligned to the spectrometer. The small prism which directs the light into the two cameras is also adjustable in the two dimensions perpendicular to this view.

The two planar mirrors are coated with an enhanced aluminum coating with reflectivity greater than 90% over the 300 to 800 nm wavelength range. Rather than use two separate pieces for the second mirror, it is actually a small prism with 15 mm square faces. The overall cost in light throughput due to the two mirrors is less than 19%. In principle, it would be possible to make this design work without vertically deflecting the light. However, that would require cutting a 120 mm wide slot in the body of the spectrometer so that portions of the CCD camera bodies could fit into this slot. Given that the spectrometers were already made and fully aligned, we considered this to be too major a step. Drilling a hole in the removable hatch cover was much simpler.

Another improvement that was made in the overall system was improved focusing of the Czerny-Turner spectrometers. A standard Czerny-Turner design contains two spherical mirrors; one collimates the light going to the grating and the other focuses the wavelength-dispersed light from the grating back down to the exit plane. However, because of spherical aberration in the mirrors, the planes of best tangential (wavelength-direction) and sagittal (vertical) focus are not the same; they are displaced about 12 mm and inclined relative to each other about one degree in the Acton AM506 spectrometers that we use. Because the CCD detector must be put at the tangential focus for the optimum wavelength resolution, the vertical blurring increases the amount of detector height that must be devoted to the image of pair of fibers positioned at the entrance slit. In our previous work,[21] we compensated for this effect by moving the tip of the fiber back 12 mm from the entrance slit. Since the horizontal extent of the image is defined by the slit while the vertical extent is defined by the top and bottom of the optical fiber, this

essentially makes the two focal planes coincident at the exit region of the spectrometer. However, without any other optics at the entrance slit, calculations indicate that this configuration costs about a factor of 2.7 in light coupling from the fiber to the spectrometer for the 1.5 mm core diameter fiber used previously;[21] the lost light impacts the jaws of the slit and is cut off. (This loss would have been a factor of 4.4 for the 0.75 mm core diameter pairs used in the edge system.) We compensated for this loss partially by positioning two vertically oriented planar mirrors on either side of the slit separated by about 1 mm. In the horizontal direction, these form a light guide. The mirrors were coated with aluminum and overcoated with magnesium fluoride. However, for reasons not yet fully understood, we only got an enhancement of about a factor of 1.5–1.6 over the case without the double mirrors in place, which is well short of the theoretical factor of 2.7.

A more elegant solution for the spherical aberration problem is to make the first, collimating mirror in the spectrometer a toroidal mirror. By properly designing the vertical and horizontal curvatures of the mirror, the tangential and sagittal focal planes can be brought together. The planes actually meet along a line owing to their inclination; however, because the inclination is small, the focus is good over the entire 7.82 mm width of our Pluto CCD detector. These mirrors were designed, fabricated and installed by Acton[23] on the spectrometers used with our older[21] and more recent CCD detectors. Tests with the older detectors indicate about a factor of two improvement in light throughput compared to the case with the double planar mirrors. This design is also significantly easier to align to the entrance slit, since the optical fibers can be butted directly up against the slit with no need to adjust the double mirror location.

Our Acton spectrometers are usually operated with 1800 g/mm gratings. This gives sufficient dispersion that we can use 300 micron wide slits while still being able to separate the important lines near C~VI 529.05 nm. The Acton spectrometers are designed for zero coma at 300 nm wavelength setting with this grating. Coupling this with the relatively wide slit widths means that coma is not really a problem for our system.

The improvements in signal and signal to noise over the intensifier-based system can be estimated straightforwardly from the parameters of the different spectrometers and detectors. The signal per pixel on each of the detectors is proportional to DQ/f^2, where f is the spectrometer f/number, D is the dispersion in pm/pixel and Q is the quantum efficiency. The Acton spectrometers are f/4.7 while the older Spex spectrometers are f/6.8. The quantum efficiency of the PixelVision CCD is at our typical 529.05 nm wavelength is 0.75 while that of the ITT image intensifiers is 0.1. Finally, we are binning the serial output of the PixelVision camera by two so that our spectra effectively contain 326 pixels which are 24 microns wide; this contrasts with the 25 micron wide pixels of the Reticon linear diode arrays. Coupled with the parameters of the spectrometers, this gives a dispersion of 15.6 pm/pixel for the new system versus 11.62 pm/pixel

for the intensifier-based system. Accordingly, we calculate an improvement of a factor of 21 in the photoelectrons per pixel on the detector with the PixelVision cameras.

In estimating the improvement in signal to noise, we must take three factors into account. First, of course, is the standard photon statistics noise in which the variance is equal to the mean number of photoelectrons. Second, there is the effective read noise of the detectors. This must be expressed in equivalent photoelectrons at the first photocathode for the intensifier-based system. Finally, there is an increase in the photon statistics noise for the intensifier by about a factor of 1.8 owing to the details of the amplification process in the intensifier. This means the photon statistics variance for the intensifier system needs to be multiplied by $1.8^2 = 3.24$. Accordingly, the noise for the CCD system is $(S_e + r_e^2)^{1/2}$ while that for the intensifier-based system is $(3.24S_e + r_e^2)^{1/2}$. Here, S_e is the signal in photoelectrons and r_e is the effective read noise in electrons. There are two simple limits to the signal to noise calculation. For very low signal levels, the readout noise dominates the noise and so the ratio of the signal to noise between CCD and intensifier-based systems is just the signal ratio divided by the readout noise ratio. For TDI mode, this turns out to be about 2 while for sample mode it is about 4. (A similar low signal calculation for our older CCD detector would give about 0.8, indicating that the intensifier-based system is actually slightly superior to that CCD in low signal cases.) The other simple limit is the large signal limit where the noise is dominated by photon statistics; in this case, the ratio of signal to noise for the two systems is 1.8 times the square root of the signal ratios. This is about 8 for both TDI and sample readout modes.

In addition to the hardware to couple the Pluto cameras to the spectrometers, considerable software work had to be done to integrate them into the overall CER data acquisition system and to modify the CER analysis codes to utilize the data from the new detectors. The basic subroutines from PixelVision which interface with the camera are written for a Windows environment while the rest of our system is Unix-based.

An unexpected problem with the Pluto cameras was a changing background level which occurs at the start of a set of external trigger pulses or when the interval between these pulses is changed. When the cameras are not being externally triggered, they idle in a so-called flush cycle in which one row is clocked onto the serial register and then this register is read out; this dumps dark current. The digitizer is not active during this cycle so none of this dark current is recorded in PC memory. When we switch to TDI mode, for example, the change in the readout apparently causes changes in dark current which can take tens of seconds to stabilize. A similar change occurs when the integration time is varied part way through a set of trigger pulses, although it usually only takes a fraction of a second for this change to stabilize. Such a change in trigger interval occurs, for example, when the experimentalists want to cover different part of the shot with different time resolution. To minimize the overall DC level change, we implemented control electronics which would externally trigger the cameras repetitively at 10 ms intervals during the

time between tokamak shots. This trigger was inhibited and the standard, shot-synchronous triggers used during the tokamak shot. In addition, we have found it necessary to take a complete sequence of data without light using the same timing as a tokamak shot in order to allow proper background subtraction in cases with multiple integration times during one shot.

This background level drift has also propagated into our analysis of the spectra from the wavelength calibration lamps[27] which we use to establish the zero of rotation. Because of technical constraints in taking these data, the background acquisition is taken several minutes before the actual data. Over this period of time, the background level can sometimes drift by 20 digitizer counts on some cameras. Since this drift is different for the four quadrants of the chip, the drift sometimes results in a background level offset between the left and high halves of the spectra. One of our eight cameras is much more subject to this than the others. We compensated for this in software by including different background levels in the least squares fitting for the spectra on the two halves of the chip. We have not seen an effect like this in the tokamak data where the background and the data are taken within a few seconds of each other.

II. TOKAMAK RESULTS

Four AM506 spectrometers equipped with eight Pluto cameras were ready for the start of the 2000 experimental campaign in January, 2000. As an initial check of the time response of the system, we examined the Doppler shifted D_α radiation from the full energy deuterium neutral beam particles in a case where the beam was modulated on and off. Previous measurements show that the beam turn on time is about 100 microseconds while the beam turn off time is about 60 microseconds. The results are shown in Fig. 3 where we plot the intensity of the signal at the wavelength of peak emission versus time. As can be seen by comparing with the neutral beam voltage waveform, at 0.33 ms integration time we are able to follow the beam turn on and off rather well. The extra structure on the D_α waveform relative to the beam voltage is due to evolution of the discharge in the neutral beam ion source as well as changes in the edge plasma.

A comparison between the intensifier-based system, our previous CCD detectors[21] and the present detectors is shown in Fig. 4. Here we have plotted the signal from one pixel on each detector as a function of time in a case where the spectrometers are tuned to the C VI 529.05 nm line and the neutral beams are modulated 10 ms on, 10 ms off. The pixel chosen for each case is near the peak of the C VI line. The signal from the intensifier-based system is visibly noisier than that from the CCD. The PixelVision measurement here is done using TDI mode with software serial binning; this increases the noise by a factor of $2^{1/2}$ over hardware binning. The CCDs follow the beam modulation more accurately than the intensifier system does, owing to the finite lifetime of the P-20 phosphor in the intensifier. The first timeslice after the beam turns on has a low signal because the beam turn on is about 0.2 ms to 0.3 ms after the start of the CCD integration time.

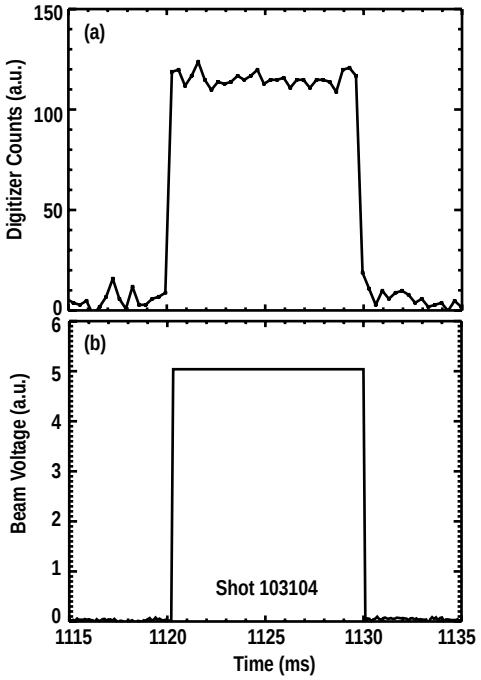

Fig. 3. (a) Time history of signal in one pixel on the detector located near the peak of the Doppler shifted D_α emission from the full energy component of a modulated neutral beam. CCD integration time is 0.33 ms. (b) Neutral beam voltage waveform showing the beam modulation. This is digitized with 0.1 ms time resolution.

An example of analyzed data from the PixelVision detectors is shown in Fig. 5. Here, we

have plotted the signal intensity, toroidal rotation speed and ion temperature determined from the spchanges ectra in a plasma where edge localized modes (ELM) and MHD oscillations are causing in the edge on a short time scale. These data are taken in a case where the two neutral beams viewed by this chord are modulated out of phase. The beam modulation is nominally 10 ms on, 10 ms off; however, one beam takes between 0.2 ms and 0.3 ms to turn on after being triggered while the other takes about 0.5 ms. The beams do go off exactly when triggered to within about 0.06 ms. Accordingly, there is no signal in the integration times which overlap the 0.5 ms delay period and there is reduced signal in the integration times which overlap the period when the other beam is partially on. This is reason for the low signal at 10 ms intervals in Fig. 5(a). Being able to track this change is another indication of the good time resolution of the CCD cameras.

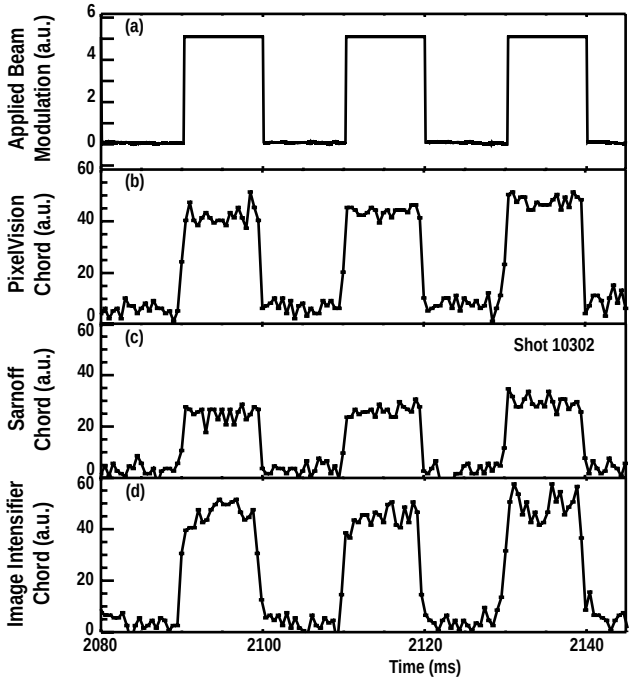

Fig. 4. Comparison of the C VI signal from one pixel of (a) one of the new PixelVision cameras, (b) one of the older CCD cameras [21] and one of the intensifier-based detectors. In (a) and (b), the integration time is 0.5 ms while in (c) it is 0.52 ms. Also shown is the neutral beam voltage waveform in (d) digitized at 0.1 ms intervals.

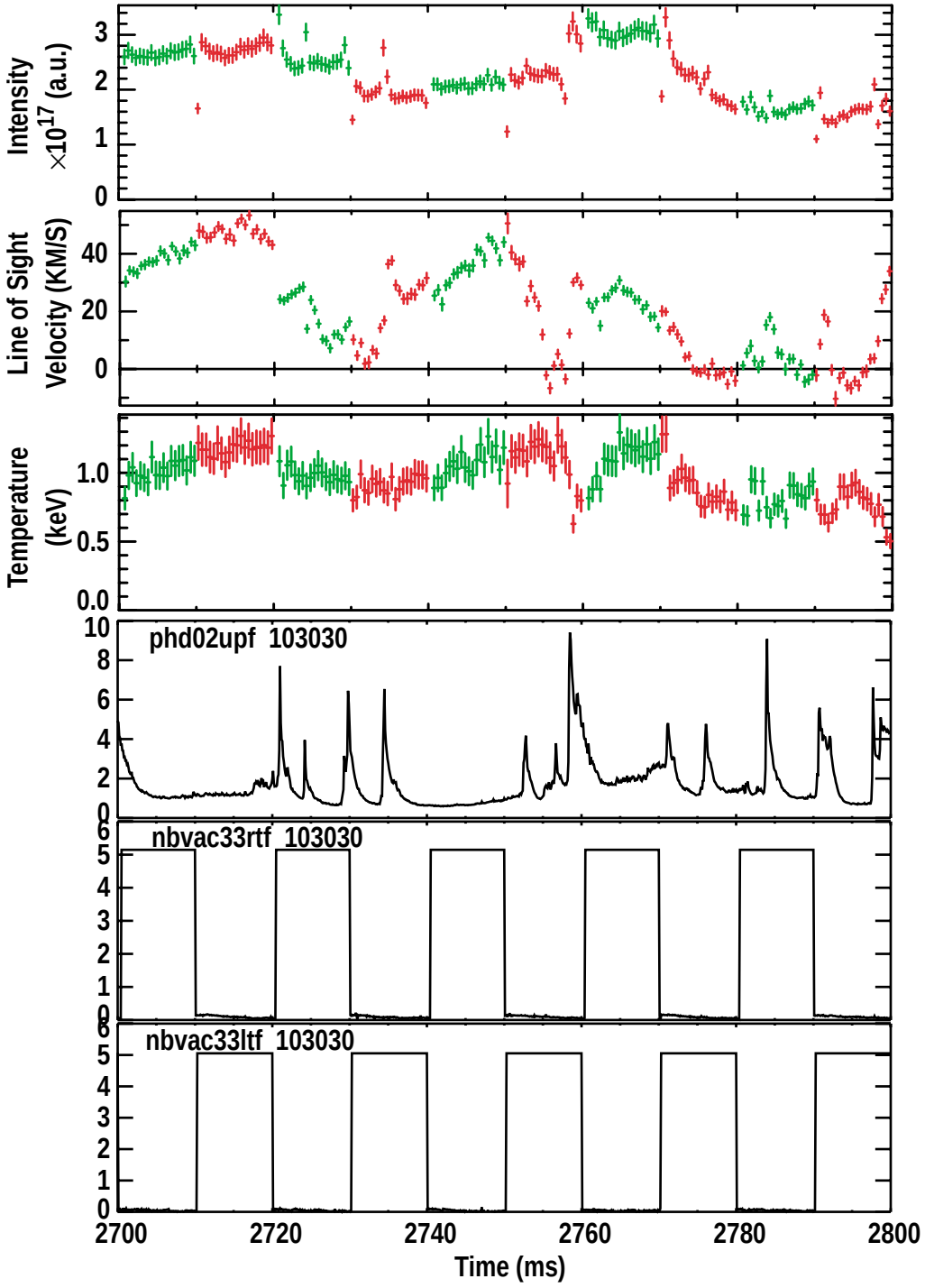

Fig. 5. Changes in (a) signal intensity (b) carbon toroidal rotation speed and (c) ion temperature associated with ELMs at the plasma edge. The ELMs are shown in (d) which is the D_α emission from the plasma edge. The integration time for the PixelVision camera was 0.5 ms for these data. The neutral beam voltage waveform is shown for the (e) 330RT beam and (f) 330LT beam.

REFERENCES

[a]Lawrence Livermore National Laboratory, Livermore, California.

[1]R.C. Isler, Phys. Rev. Lett. **30**, 1359 (1977).

[2]R.J. Fonck, D.S. Darrow, and K.P. Jaehnig, Phys. Rev. A **29**, 3288 (1984).

[3]R.J. Groebner, N.H. Brooks, K.H. Burrell, and L. Rottler, Appl. Phys. Lett. **43**, 920 (1983).

[4]R.J. Fonck, R.J. Goldston, R. Kaita, and D. Post, Appl. Phys. Lett. **42**, 239 (1983).

[5]R.P. Seraydarian and K.H. Burrell, Rev. Sci. Instrum. **57**, 2012 (1986).

[6]R.P. Seraydarian, K.H. Burrell, R.J. Groebner,, Rev. Sci. Instrum. **59**, 1530 (1988).

[7]K. Ida and S. Hidekuma, Rev. Sci. Instrum **60**, 867 (1989).

[8]A. Boileau, M. von Hellermann, L.D. Horton, and H.P. Summers, Plasma Phys. Control. Fusion **31**, 779 (1989).

[9]R.J. Groebner, K.H. Burrell and R.P. Seraydarian, Phys. Rev. Lett. **64**, 3015 (1990).

[10]R.J. Groebner, Rev. Sci. Instrum. **61**, 2920 (1990).

[11]P. Gohil, K.H. Burrell, R.J. Groebner, and R.P. Seraydarian, Rev. Sci. Instrum. **61**, 2949 (1990).

[12]M. von Hellermann, W. Mandl, H.P. Summers, H. Weisen, A. Boileau, P.D. Morgan, H. Morsi, R. Konig, M.F. Stampf, and R. Wolf, Rev. Sci. Instrum. **61**, 3479 (1990).

[13]K. Ida, H. Yamada, H. Iguchi, K. Itoh, and CHS Group, Phys. Rev. Lett. **67**, 58 (1991).

[14]P. Gohil, K.H. Burrell, R.J. Groebner, J. Kim, W.C. Martin, E.L. McKee, and R.P. Seraydarian, in Proceedings of the Fourteenth IEEE/NPSS Symposium on Fusion Technology (IEEE, Princeton, 1992), Vol II, p. 1199.

[15]Y. Koide, M. Kikuchi, M. Mori, S. Tsuji, S. Ishida, N. Asakura, Y. Kamada, T. Nishitani, Y. Kawano, T. Hatae, T. Fujita, T. Fukuda, A. Sakasai, T. Kondoh, R. Yoshino, and Y. Neyatani,Phys. Rev. Lett **72**, 3663 (1994).

[16]R.E. Bell, L.E. Dubek, B. Grek, D.W. Johnson, and R.W. Palladino, Rev. Sci. Instrum. **70**, 821 (1999).

[17]K.H. Burrell, E.J. Doyle, P. Gohil, R.J. Groebner, J. Kim, R.J. La Haye, L.L. Lao, R.A. Moyer, T.H. Osborne, W.A. Peebles, C.L. Rettig, T.L. Rhodes, and D.M. Thomas, Phys. Plasmas **1**, 1536 (1994).

[18]K.H. Burrell, E.J. Strait, L.L. Lao, M.E. Mauel, B.W. Rice, T.S. Taylor, T.A. Casper, B.W. Stallard, E.A. Lazarus, and T.H. Osborne, Plasma Physics and Controlled Nuclear Fusion Research 1994 (IAEA, Vienna, 1995), Vol 1, p. 221.

[19]R.A. Moyer, K.H. Burrell, T.N. Carlstrom, S. Coda, R.W. Conn, E.J. Doyle, P. Gohil, R.J. Groebner, J. Kim, R. Lehmer, W.A. Peebles, M. Porkolab, C.L. Rettig, T.L. Rhodes, R.P.

Seraydarian, R.E. Stockdale, D.M. Thomas, G.R. Tynan, and J.G. Watkins, Phys. Plasma **2**, 2397 (1995).
[20]R.J. Groebner, T.H. Osborne, Phys. Plasmas **5**, 1800 (1998).
[21]D.M. Thomas, K.H. Burrell, R.J. Groebner, P. Gohil, D.H. Kaplan, C.C. Makariou, and R.P. Seraydarian, Rev. Sci. Instrum. **68**, 1233 (1997).
[22]PixelVision, Tigard, Oregon 97223. www.pv-inc.com.
[23]Acton Research Corp., Acton, MA 01720. www.acton-research.com.
[24]Sarnoff Corporation, Princeton, NJ 08543. www.sarnoff.com
[25]M.R. Wade, T.C. Luce, C.C. Petty, Phys. Rev. Lett **79**, 419 (1997).
[26]C.C. Petty, M.R. Wade, J.E. Kinsey, R.J. Groebner, T.C. Luce, and G.M. Staebler, Phys. Rev. Lett. **83**, 3661 (1999).
[27]P. Gohil, K.H. Burrell, R.J. Groebner, K. Holtrop D.H. Kaplan, and P. Monier-Garbet Rev. Sci. Instrum **70**, 878 (1999).

ACKNOWLEDGMENTS

This work was supported by the U.S. Department of Energy under Contract Nos. DE–AC03-99ER54463 and W-7405-ENG-48. The authors wish to thank T.C. Simonen, R.D. Stambaugh, T.S. Taylor and R.T. Snider for their continuing support during this development effort. We thank K. Young at Princeton Plasma Physics Laboratory for providing the lead and borated polyethylene used in the radiation shielding.